PCCP

Physical Chemistry Chemical Physics

www.rsc.org/pccp

Volume 14 | Number 33 | 7 September 2012 | Pages 11559–11854

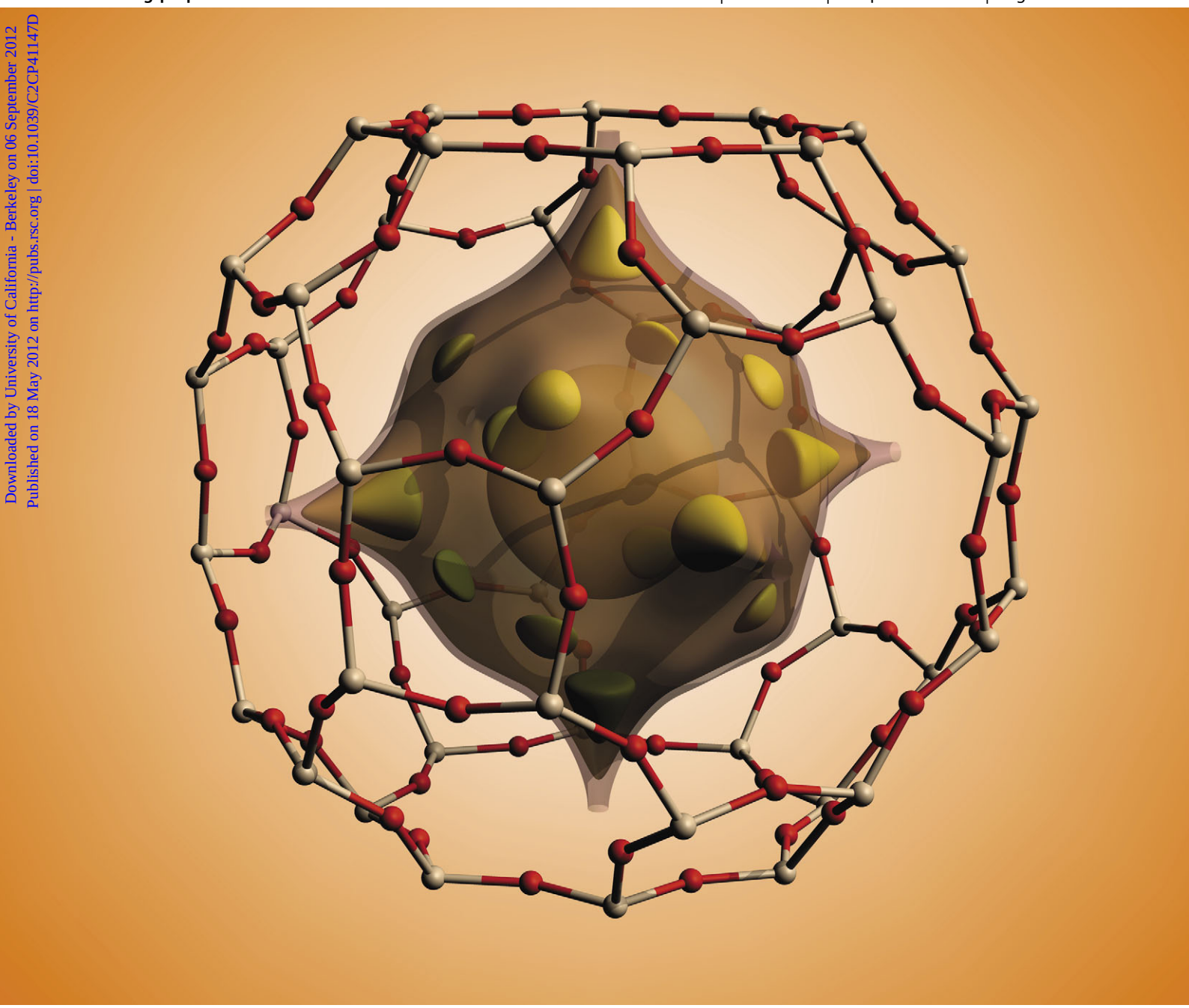

ISSN 1463-9076

COVER ARTICLE
Abouelnasr and Smit
Diffusion in confinement: kinetic simulations of self- and collective diffusion behavior of adsorbed gases

1463-9076(2012)14:33;1-Q

PCCP

Dynamic Article Links
View Online

Cite this: *Phys. Chem. Chem. Phys.*, 2012, **14**, 11600–11609

www.rsc.org/pccp

PAPER

Diffusion in confinement: kinetic simulations of self- and collective diffusion behavior of adsorbed gases†

Mahmoud K. F. Abouelnasr[a] and Berend Smit*[bc]

Received 11th April 2012, Accepted 18th May 2012
DOI: 10.1039/c2cp41147d

The self- and collective-diffusion behaviors of adsorbed methane, helium, and isobutane in zeolite frameworks LTA, MFI, AFI, and SAS were examined at various concentrations using a range of molecular simulation techniques including Molecular Dynamics (MD), Monte Carlo (MC), Bennett–Chandler (BC), and kinetic Monte Carlo (kMC). This paper has three main results. (1) A novel model for the process of adsorbate movement between two large cages was created, allowing the formulation of a mixing rule for the re-crossing coefficient between two cages of unequal loading. The predictions from this mixing rule were found to agree quantitatively with explicit simulations. (2) A new approach to the dynamically corrected Transition State Theory method to analytically calculate self-diffusion properties was developed, explicitly accounting for nanoscale fluctuations in concentration. This approach was demonstrated to quantitatively agree with previous methods, but is uniquely suited to be adapted to a kMC simulation that can simulate the collective-diffusion behavior. (3) While at low and moderate loadings the self- and collective-diffusion behaviors in LTA are observed to coincide, at higher concentrations they diverge. A change in the adsorbate packing scheme was shown to cause this divergence, a trait which is replicated in a kMC simulation that explicitly models this behavior. These phenomena were further investigated for isobutane in zeolite MFI, where MD results showed a separation in self- and collective- diffusion behavior that was reproduced with kMC simulations.

1. Introduction

Microporous materials like zeolites and, more recently, Metal–Organic Frameworks (MOFs) have been the focus of much attention in recent years because of their industrially useful properties. Of particular interest are these materials in the context of gas separations.[1–4] Microporous materials have the potential to exhibit extremely favorable separation properties due in part to the capability of closely matching the diameter of a rate-limiting diffusion pathway in the material to that of an adsorbed molecule, resulting in a "molecular sieve" action.[5]

The measurement of diffusion properties poses a problem for someone wishing to quickly scan the millions of hypothetically possible materials[6,7] for a candidate material to use in a particular separation process. Molecular simulations provide a promising route; however the benchmark technique for obtaining the diffusion coefficients of gases in these materials, Molecular Dynamics (MD), is often too slow to efficiently generate particle trajectories over the time-scales necessary to characterize the diffusion properties.[8] In particular, for systems that display the potentially useful "molecular sieve" trait, MD can be especially time consuming. For these systems, the diffusion phenomenon can often be viewed as a hopping process between large cages separated by narrow windows. June *et al.*[9] proposed an application of the Transition State Theory (TST)[10] with the Bennett–Chandler method[11,12] to model diffusion in confinement, considering adsorbate movement as uncorrelated hops on a lattice of adsorption sites and calculating the self-diffusion coefficient D_S.

Beerdsen *et al.*[13] used this method to successfully replicate the self-diffusion coefficient values found from a Molecular Dynamics simulation. In that article, the Canonical Monte Carlo and Bennett–Chandler simulations were executed in a system where the microscopic concentration was allowed to vary, but the global concentration was fixed. This resulted in an "implicit" treatment of inter-particle interactions, where an adsorbate is assumed to be subject to an effective force field comprised of all other particles in all possible configurations,

[a] *Department of Chemical and Biomolecular Engineering, University of California - Berkeley, 201 Gilman Hall, Berkeley, CA 94720-1462, United States. E-mail: forrest.a@berkeley.edu; Fax: 510-642-4778; Tel: 510-643-9800*
[b] *Department of Chemical and Biomolecular Engineering, University of California - Berkeley, 201 Gilman Hall, Berkeley, CA 94720-1462, United States*
[c] *Department of Chemistry, University of California - Berkeley, 419 Latimer Hall, Berkeley, CA 94720-1460, United States. E-mail: Berend-Smit@Berkeley.edu; Fax: 510-642-4778; Tel: 510-642-4778*

† Electronic supplementary information (ESI) available: Structure files for frameworks LTA, MFI, SAS, and AFI, as well as blocking information for framework LTA. See DOI: 10.1039/c2cp41147d

weighted by the probability of each configuration. While this approach was shown to accurately predict the self-diffusion coefficient at a range of concentrations, the collective-diffusion coefficient cannot be obtained using those means.

Krishna *et al.*[14] formed a model of the collective-diffusion behavior. Their application of the Reed-Ehrlich model[15] of diffusion on a lattice results in a reasonable fit to the collective-diffusion coefficients found from MD, using an adjustable parameter. Although this method gives important insights, it should be noted that, since it requires prior knowledge of the desired property, that method is not aimed to *predict* the collective-diffusion coefficient.

The approach of this paper is to use a kinetic Monte Carlo (kMC) simulation,[16] which, like an MD simulation, generates a set of particle trajectories that can be analyzed to calculate the desired collective-diffusion coefficient, but which can have an advantage over MD in computational speed. Starting with the formulation laid out by Beerdsen *et al.*,[13] we calculated the TST hop rates and re-crossing coefficients. However, where Beerdsen *et al.* computed the average hopping rates of a single particle as a function of global concentration, we computed these hop rates in the case where the exact loading of the participating cages is controlled. This is similar to the approach of Jee and Sholl,[17] who investigated the effect on hop rate of local cage occupancy, rather than global concentration. Calculation of these loading-specific hop rates required the development of a model to predict the re-crossing coefficient in the case of a hop between two cages of different loadings. Next, this approach was used to analytically calculate the self-diffusion coefficient while explicitly accounting for fluctuations in cage loading, allowing a comparison to previous methods. These values were then used in a subsequent kMC simulation to calculate the self- and collective-diffusion coefficients.

Building on these insights, some of the theoretical approaches developed in the methane/LTA model were tested in a variety of other systems, including methane in zeolite SAS, helium in zeolite AFI, and isobutane in zeolite MFI.

The rest of the paper is divided into three parts. First, the theoretical basis for this work is laid out, including a mixing rule for the re-crossing coefficient and a method to explicitly account for microscopic density fluctuations. Next, the simulation details are enumerated to allow reproduction of the data presented in this work. Finally, results of those simulations are presented.

2. Theory

Let us first give a short review of the dynamically corrected Transition State Theory (dcTST) of Dubbeldam and co-workers.[13,18–20] The idea of this method is to consider a tagged particle and to compute the hopping rate of this particle from one site in the zeolite to another. This hopping rate is obtained from the free energy profile and the re-crossing coefficient using standard rare-event simulation techniques.[21] In this method the contributions of the other particles is reflected in the loading dependence of these free energies and re-crossing coefficients. The resulting single-particle effective hop rate can be directly converted into the loading dependent self-diffusion coefficient. The importance of this method is that we now can compute the loading dependence of the self-diffusion coefficient for those molecules for which the diffusion is too slow for straightforward Molecular Dynamics. A limitation of this method is, however, that it does not give us information on the loading dependence of the collective-diffusion coefficients, which are important from a practical point of view.

In this work we propose an extension of the method of Dubbeldam and co-workers, which allows us to estimate the particle hopping rates that can be used in a kinetic Monte Carlo (kMC) simulation to obtain some insights in the collective-diffusion coefficients. At this point it is important to note that, similar to the approach of Dubbeldam and co-workers, the significance of our method is that it can be applied to systems for which molecular dynamics is too slow. The reason that we focus here on a system where molecular dynamics can also be used is that it allows us to validate our approach.

From a kMC simulation one can obtain the collective-diffusion coefficients directly. The difficulty is, however, to relate the hopping rates to the underlying molecular model. Dubbeldam and co-workers achieve this by considering a *single* particle hopping on this lattice but with an effective hopping rate that exactly captures the loading dependence of a tagged particle and hence can only be used for the self-diffusion coefficient. Alternatively, one can carry out a kMC simulation with exactly the number of particles at the loading of interest. However, this requires a method to obtain these hopping rates from our underlying molecular model.

Let us consider a system in which the low free-energy adsorption sites are separated by sufficiently high free-energy barriers that hopping between one site and the other can be seen as a rare event. We also consider the case that there can be several low free-energy sites close to each other. As a consequence the molecules can make many jumps between those low energy sites before jumping over the large barrier. If this is the case we assume that we have a single site but that this site can be occupied by more than one molecule. We now carry out a simulation at a given loading and use the techniques described by Dubbeldam and co-workers to compute the free energy profiles. Instead of computing the free energy profiles for this average loading $\langle m \rangle$ molecules per cage, we compute the free energy profile for a specific loading and we assume that these free energy profiles are independent of the loadings of other cages. From these free-energy profiles we can compute the transition state hopping rates. The re-crossing coefficients, for a particle moving between cages, we compute using the assumption that the probability a particle, upon entering a cage, is bounced back out the way it came depends only on the loading of that cage (see Section 2.3). With these assumptions we can obtain a set of hopping rates. From these hopping rates we can calculate both the self-and collective-diffusion coefficients from a kinetic Monte Carlo simulation.

2.1 Transition state theory hop rates

Transition State Theory, as applied to this system, assumes that any particle that reaches the window between cages

(a free-energy maximum) will move from one cage to the other. The average hop rate can then be calculated as

$$k_{A\to B} = \nu_B \times \frac{e^{-\beta F(\text{barrier})}}{\int_{\text{cage A}} e^{-\beta F(x)} dx}, \quad (1)$$

where ν_B is the average magnitude of the velocity as obtained from the Boltzmann distribution, $F(x)$ is the Helmholtz Free Energy of a particle at with order parameter x defined by its position, and k_B is Boltzmann's constant.

2.2 Re-crossing coefficient

TST assumes that all particles that arrive at the free energy barrier hop successfully. In these systems, however, the geometry of the material or the presence of other particles can cause a particle with a positive velocity to re-cross the transition state. These effects require a correction of the TST results, the re-crossing coefficient. This re-crossing coefficient can be calculated using a Bennett–Chandler simulation for any arbitrary loading of either cage, as described in Section 3.4. This coefficient can be interpreted as the conditional probability that a particle will hop from one cage to another, given that the particle is on the free-energy barrier between the cages. The resulting dynamically corrected hop rate is given by

$$K_{\text{dcTST}} = K_{\text{TST}} \times \kappa = \nu_B \times \frac{e^{-\beta F(\text{barrier})}}{\int_{\text{cage}} e^{-\beta F(x)} dx} \times \kappa,$$

where κ is the re-crossing coefficient. However, the applicability of the resulting hop rate depends on the particular constraints imposed on the system when collecting the data that goes into the equation. For example, if the global concentration is fixed, but the loading in each cage is allowed to fluctuate naturally (*e.g.* by having a constant total number of particles, but a relatively large system), then the resulting hop rate will be the average hop rate. In this case the self-diffusion coefficient D_S on a cubic lattice like that of LTA, can be calculated directly as[22]

$$D_S^{\langle n\rangle} = \lambda^2 \times K_{\text{hop}}^{\langle n\rangle} \times \kappa^{\langle n\rangle}, \quad (2)$$

where λ is the cage-to-cage distance, $\langle n\rangle$ is the average number of particles per cage, and K_{hop} is the TST hop rate as defined by eqn (1), with the superscripts denoting the simulation conditions. The corrected hop rates provided by this formulation cannot be applied to a kinetic Monte Carlo simulation to measure the collective-diffusion coefficient, since the interactions between particles are accounted as an average effect; the effects of fluctuations are averaged. Before detailing our solution to this problem, it is first necessary to discuss the re-crossing coefficient for asymmetrical loadings.

2.3 Re-crossing coefficient for asymmetrical loadings

Here we will derive an expression to estimate the re-crossing coefficient between two cages of unequal loading from the re-crossing coefficients calculated at equal loadings. Let us first consider a particle observed on the barrier between two cages A and B, which have respective loadings i and j, and the particle is currently moving toward cage B. We assume that the probability $P_b(j)$ that a particle, upon entering a cage, is bounced back out the way it came, depends only on the loading j of that cage. The probability that this particle will end up in cage B is therefore

$$\begin{aligned} P_{\text{end in B}} &= (1 - P_b(j)) + P_b(j)P_b(i)(1 - P_b(j)) + \cdots \\ &= (1 - P_b(j)) \times \sum_{x=0}^{\infty} (P_b(j)P_b(i))^x \\ &= \frac{1 - P_b(j)}{1 - P_b(j)P_b(i)} \end{aligned} \quad (3)$$

by simplifying the geometric series. Similarly, the probability that the particle ends up in cage A is

$$P_{\text{end in A}} = \frac{P_b(j)(1 - P_b(i))}{1 - P_b(i)P_b(j)}. \quad (4)$$

Because the model system behaves the same whether the system is moving forward or backward in time, the probability that the particle started in cage A can be calculated similarly as

$$P_{\text{start in A}} = \frac{1 - P_b(i)}{1 - P_b(j)P_b(i)}, \quad (5)$$

and likewise the probability that the particle started in cage B can be calculated as

$$P_{\text{start in B}} = \frac{P_b(i)(1 - P_b(j))}{1 - P_b(i)P_b(j)}. \quad (6)$$

Defining a transmission probability as the conditional probability that a particle starts in cage A and ends in cage B is hence the product of eqn (5) and (6):

$$P(A \to B) = P_{\text{start in A}} \times P_{\text{end in B}}. \quad (7)$$

The re-crossing coefficient is then the normalized net flux across the barrier is now

$$\kappa_{ij} = \frac{P(A \to B) - P(B \to A)}{P(A \to B) + P(B \to A) + P(A \to A) + P(B \to B)}. \quad (8)$$

Setting $i = j$ and substituting eqn (3)–(7) into eqn (8) yields

$$\kappa_{ii} = \frac{1 - P_b(i)^2}{1 + 2P_b(i) + P_b(i)^2}. \quad (9)$$

Solving quadratically for $P_b(i)$, and noting that $P_b(i)$ must be non-negative, yields

$$P_b(i) = \frac{1 - \kappa_{ii}}{1 + \kappa_{ii}} \quad (10)$$

which, when substituted into eqn (3)–(8), gives the final mixing rule

$$\kappa_{ij} = \frac{2\kappa_{ii}\kappa_{jj}}{\kappa_{ii} + \kappa_{jj}} \quad (11)$$

Eqn (11) may be recognized as the harmonic mean. This function satisfies the necessary symmetry $\kappa_{ij} = \kappa_{ji}$, which is required for detailed balance.

2.4 Calculation of hop rates with explicit contribution from concentration fluctuations

Next will be presented a method to separate the contribution that each specific cage-loading case makes toward the mean

Table 1 Simulation parameters for zeolite framework systems

Zeolite name	Simulation box size (x) [Å]	Simulation box size (y) [Å]	Simulation box size (z) [Å]	Cut-off radius [Å]	Number of super-sites
LTA	24.555	24.555	24.555	12.0	8
SAS	28.644	28.644	20.848	10.0	16
AFI	23.774	27.452	25.452	10.0	96
MFI	40.044	39.798	26.766	12.0	32

value and re-mix them properly. For this purpose, the Canonical MC simulation results are analyzed to give the TST hop rates for the case of exactly i, rather than an average of $\langle n \rangle$, particles in a cage, through eqn (1). Next, the normalized probability $P^{\mathrm{occ},\langle n \rangle}(j)$ of observing a cage with exactly j particles in a system with on average $\langle n \rangle$ particles per cage is recorded. The related normalized probability of observing a *particle* in a cage with occupancy i in a system with average occupancy $\langle n \rangle$ per cage is defined as

$$\bar{P}^{\mathrm{occ},\langle n \rangle}(i) = \frac{i \times P^{\mathrm{occ},\langle n \rangle}(i)}{\sum_{j=0}^{\infty} j \times P^{\mathrm{occ},\langle n \rangle}(j)} \tag{12}$$

The resulting corrected hop rate is calculated as the summation over all possible hops from a cage with i particles to a cage with j particles, weighted by the probability of observing that situation in a system with $\langle n \rangle$ average particles per cage,

$$K_{\mathrm{hop}}^{\langle n \rangle} \times \kappa^{\langle n \rangle} = \sum_{i=1}^{\infty} \sum_{j=0}^{\infty} \bar{P}^{\mathrm{occ},\langle n \rangle}(i) \times P^{\mathrm{occ},\langle n \rangle}(j) \times K_{\mathrm{hop}}^{i} \times \kappa_{i-1,j} \tag{13}$$

Combined with eqn (2), (11), and (12), this allows an explicit calculation of the self-diffusion coefficient as

$$D_{\mathrm{S}}^{\langle n \rangle} = \lambda^2 \sum_{i=1}^{\infty} \sum_{j=0}^{\infty} \bar{P}^{\mathrm{occ},\langle n \rangle}(i) \times P^{\mathrm{occ},\langle n \rangle}(j) \times K_{\mathrm{hop}}^{i} \times \kappa_{i-1,j} \tag{14}$$

It should be noted that the re-crossing coefficients used in eqn (13) and (14) account for the fact that one particle, the one executing the hop, is no longer in its original cage at the time of the calculation.

2.5 Kinetic Monte Carlo

Now the groundwork is laid for a kinetic Monte Carlo simulation. The only necessary inputs for such a simulation are the lattice topology and the rates at which hop events occur. The hop rate of a particle from its current cage A into a neighbor cage is given by

$$k_{\mathrm{hop}} = \nu_{\mathrm{B}} \times \frac{\mathrm{e}^{-\beta F(\mathrm{barrier})}}{\int_{\mathrm{cage}} \mathrm{e}^{-\beta F(x)} \mathrm{d}x} \times \frac{2\kappa_{ii}\kappa_{jj}}{\kappa_{ii} + \kappa_{jj}}, \tag{15}$$

where i is the loading of the origin cage (not including the hopping particle), j is the loading of the destination cage, and statistics for the free energies are collected from a simulation with exactly i particles in the cage. Once these values are tabulated, a kinetic Monte Carlo simulation can be run which faithfully recreates some aspects of the diffusion behavior.

3. Simulation methodology

3.1 Simulation system

Here we describe the simulations systems used for MD, MC, and Bennett–Chandler simulations. Methane and isobutane pseudo-atoms (elsewhere referred to as "united-atoms") were simulated using the Lennard-Jones (LJ) parameters described by Dubbeldam *et al.*,[23,24] and helium atoms were simulated with the LJ parameters reported by Talu and Myers.[25] Simulation details of the zeolite frameworks are enumerated in Table 1. The all-silica zeolite frameworks[19,26] † were assumed to be rigid, so to enhance computational efficiency the truncated and shifted LJ potential energy between an adsorbate pseudo-atom and all oxygen atoms of the framework was tabulated for a grid of resolution 0.15 Å in the simulation box. During the simulation the LJ interactions between an adsorbate and the framework were found by cubic spline from this lookup table. Adsorbate–adsorbate interactions were calculated by directly evaluating the truncated and shifted Lennard-Jones potential during the simulation. Periodic Boundary Condition (PBC) was used and inaccessible pores in the zeolite were blocked by prohibiting adsorbate entry into specified inaccessible pockets[27] †. While it has been shown in MD simulations that the simulation box size has a significant effect on the diffusion behavior in one-dimensional channel systems like SAS and AFI,[28] the short time scale of the Bennett–Chandler simulation allows an accurate determination of the re-crossing coefficient with a relatively small simulation box.

3.2 Molecular dynamics

To directly calculate the diffusion coefficients, the Canonical Ensemble (NVT) was simulated, using the Nosé-Hoover method to regulate temperature.[29,30] For part of the Bennett–Chandler simulations, the Micro-Canonical Ensemble (NVE) was simulated. Step sizes for all MD simulations were 0.5 fs. Except for the MD simulations used as part of the Bennett–Chandler simulations, MD simulations were equilibrated for 1 ns or more, and total simulation time was 20 ns or more. The Verlet Algorithm[31] was used at each time-step.

3.3 Canonical Monte Carlo

The MC simulations used the same system and potentials as described above (Sections 3.1 and 3.2). The Metropolis acceptance algorithm[32] was used to impose the temperature, with the maximum displacement tuned to achieve an acceptance ratio of 20%. Each MC simulation was run for 1.5×10^8 steps or more. The probability density of observing a particle at a given position can be calculated from a Canonical MC simulation; the coordinates of each particle are recorded at regular intervals, and sorted into planar bins that are orthogonal to the straight path between cage centers. Dividing the number of hits in each bin by the size of the bin yields the probability density for that bin $P(x)$, allowing calculation of the Helmholtz Free Energy through the relationship

$$F(x) = -RT \times \ln P(x). \tag{16}$$

3.4 The Re-crossing coefficient

Bennett–Chandler simulations[11,12] were executed by first running a Monte Carlo simulation of the Canonical Ensemble

as described above, where one particle is constrained to the Free Energy barrier plane between two adsorption sites. Uncorrelated snapshots of this system 1000 MC steps apart were used as starting points for short Micro-Canonical (NVE) MD simulations. In these MD simulations, each particle was given a random velocity sampled from the Boltzmann distribution at the given temperature. This allowed a designation of "expected donor" cage and "expected receiver" cage. Each short MD simulation was run until either the particle in question moved past the center of either cage, or 20 ps of simulation time elapsed. The re-crossing coefficient was then calculated as the normalized net flux of particles across the barrier over many such simulations (more details can be found in Frenkel and Smit[21] or Dubbeldam *et al.*[18]).

3.5 Kinetic Monte Carlo

The first LTA system consisted of a 3 × 3 × 3 lattice of super-cage sites, each of which can accommodate up to fifteen particles. The second LTA system consisted of a 3 × 3 × 3 lattice of super-cages split into 15 distinct sites, each of which could accommodate only one particle (see Fig. 7). The MFI system consisted of 32 intersection sites, with an additional 128 channel sites for the second model; each site was considered to accommodate only one molecule.

In principle it is possible to run a kMC simulation using an unvarying hop rate $K_{\text{hop}}^{\langle n\rangle} \times \kappa^{\langle n\rangle}$,but in that case a simulation is not necessary as the result converges to that of a random walk on a lattice. Furthermore, in that case there is no explicit interaction between particles, meaning that $D_C = D_S$, which does not reflect reality. Instead, the hop rates used were those for the exact loading case, $K_{\text{hop}}^{i} \times \kappa_{ij}$, explicitly accounting for microscopic fluctuations. If correctly executed, the simulated system should have the same $P^{\text{occ},\langle n\rangle}$ cage-loading distribution values as in the Canonical MC simulations, and therefore should yield the same D_S as the analytical solution above (see Section 2.4).

All kMC simulations advanced forward in time using the Gillespie Algorithm,[33] with a binary search algorithm to efficiently determine the selected event. Each kMC simulation was run for at least 100 ns, after at least a 10 ns equilibration period.

3.6 Calculation of diffusion coefficients

Each kMC or MD simulation yields an ensemble of particle trajectories. The self-diffusion coefficient can be calculated[5] as

$$D_S = \frac{1}{2d}\lim_{t\to\infty}\frac{d}{dt}\langle[r(t) - r(0)]^2\rangle, \qquad (17)$$

where r is the position of a given particle. This self-diffusion coefficient characterizes the movement of a given adsorbate. The collective-diffusion coefficient can be calculated as

$$D_C = \frac{N}{2d}\lim_{t\to\infty}\frac{d}{dt}\left\langle\left\{\frac{1}{N}\sum_{i}^{N}[r_i(t) - r_i(0)]\right\}^2\right\rangle, \qquad (18)$$

which characterizes the movement of the center of mass of all N adsorbate particles in the system. The collective-diffusion coefficient can then be used to find the molar flux as a function of the chemical potential, μ:

$$J = -D_C\nabla\mu. \qquad (19)$$

If the adsorption isotherm is known, the collective-diffusion coefficient can be converted into the Fick diffusion coefficient, which is the diffusion coefficient required in mass transfer problems in the design of industrial processes using these materials.

4. Results and discussion

4.1 Diffusion of methane in LTA

4.1.1 Transition state theory. In our method we rely on the assumption that adsorbate movement can be treated as uncorrelated hops between adsorption sites. To test this, we must first collect the hop rates of these particles between cages, which are heavily influenced by the number of particles loaded into each cage. This information could be measured in either of two systems: first, one where the global concentration is fixed, but the instantaneous loading of each super-cage is allowed to fluctuate, faithfully reproducing the system's natural fluctuations; and second, where the number of particles in each cage is constrained. Fig. 1 shows the free energy in LTA for both situations. Systematic differences can be seen between the two cases.

In our scheme we assume that movements within a cage occur on a much faster time-scale than hops between two separate cages. This requires that the free energy barriers within a cage are relatively small compared to the barriers between cages. The derivative of the Free Energy of methane in LTA at 300 K with respect to position is shown for loadings of seven, eight, nine, and ten particles per cage (Fig. 2). At a position of approximately 2 Å from the barrier, the function is observed to cross the x-axis at densities of nine particles per cage and higher. This indicates the emergence of local maxima in the probability density at those locations, marking the beginning of a new packing scheme at high densities. The shaded areas represent the depth of the local minimum in the free energy. Whereas at lower densities the particles wander around the cage relatively freely, at higher densities they are stuck, for short time scales, in a sub-cage formed in part by other pseudo-stationary adsorbates.

4.1.2 Re-crossing coefficients. The re-crossing coefficient of methane in LTA was calculated for an average loading, and

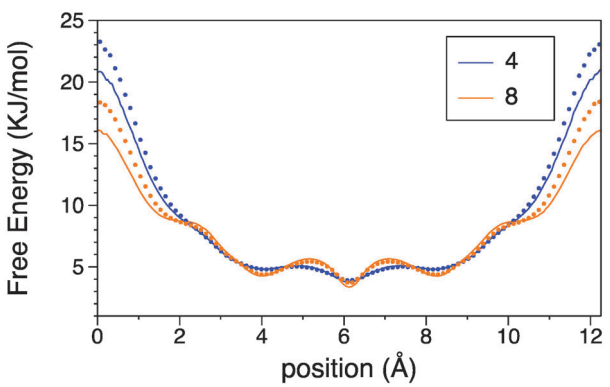

Fig. 1 Free energy of methane as a function of the position in the cage in LTA at 300 K. Lines are the result when the local concentration is allowed to fluctuate, and dots are the result when the number of particles in a cage remains fixed. The legend shows the number of particles in each cage.

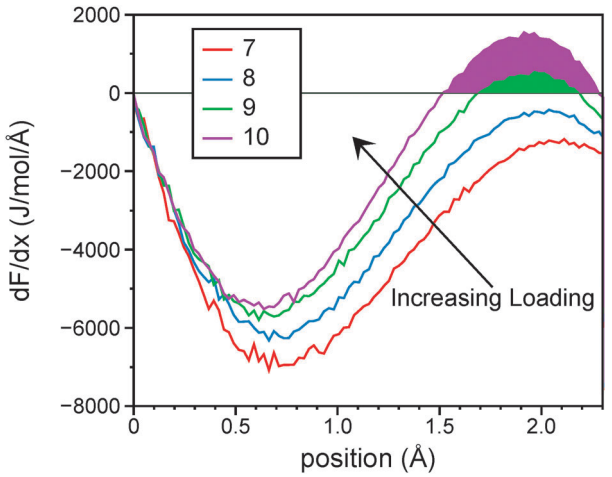

Fig. 2 The derivative of the free energy with respect to position for methane in LTA at 300 K. Loading (molecules per super-cage) is indicated in the legend.

compared to the values obtained by Beerdsen *et al.*,[19] showing quantitative agreement (Fig. 3). Lower values of the re-crossing coefficient correspond to a higher likelihood that the entering particle will be blocked by another adsorbate.

The re-crossing coefficient was then calculated for various exact asymmetrical loadings, and compared to the new model presented in this paper (Fig. 4). The model is observed to be accurate in LTA as long as both cages have fewer than nine particles per cage, with a correlation coefficient of 0.99. The breakdown of the model, starting at nine particles per cage, corresponds to the concentration where additional local maxima in the probability density start appearing (Fig. 2). This leads to adsorbate behavior that violates the core assumption of the model: that the probability of a cage to reject an entering particle is constant. If particles spend a longer amount of time stationary near the entrance of a cage than the hopping particle spends bouncing between two cages, then the probability of a rejection during the current attempt is correlated with the probability of a rejection during the last attempt; this is not accounted for in the model.

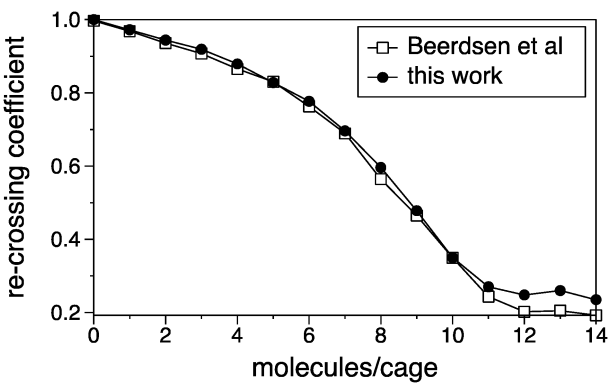

Fig. 3 Re-crossing coefficient of methane in zeolite LTA at 300 K at various average loadings. The non-participating particles are allowed to move between cages during the Canonical MC simulation, but the total number of particles in all eight cages was constant throughout each simulation.

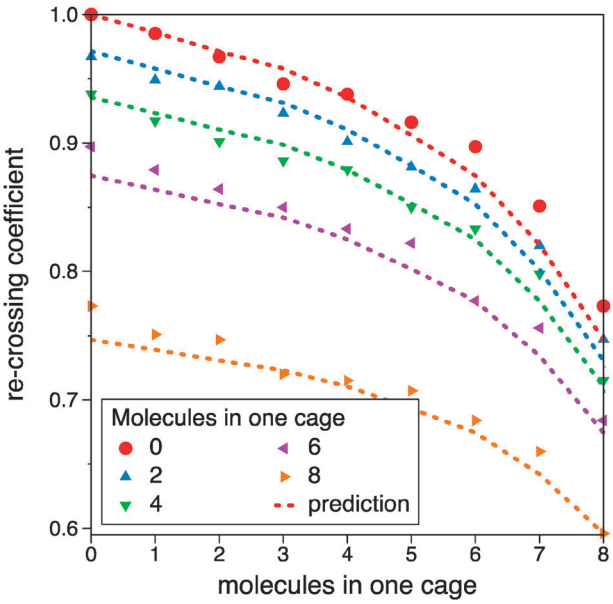

Fig. 4 Re-crossing coefficients of methane in zeolite LTA at 300 K with constrained cage loadings. The *x*-axis denotes the loading of one cage, while the legend denotes the loading of the other cage. Symbols are the observed values, while dotted lines show values predicted by the model presented in this work.

4.1.3 Analytical calculation of self-diffusion coefficient. For LTA, the probability $P^{\mathrm{occ},\langle n\rangle}$ observing a cage with i particles in a system with an average $\langle n\rangle$ particles per cage was recorded from Canonical MC simulations (Fig. 5). This probability distribution was used in the novel D_S calculation that explicitly accounts for fluctuations in concentration (presented in the Theory section). The distributions are narrower than would be predicted from non-interacting particles (not shown), indicating a free-energy penalty for higher cage loadings. The cage occupancy probability was also recorded from simulations of the first kMC model. It can be seen that the cage occupancy distributions offer precise quantitative agreement at lower average

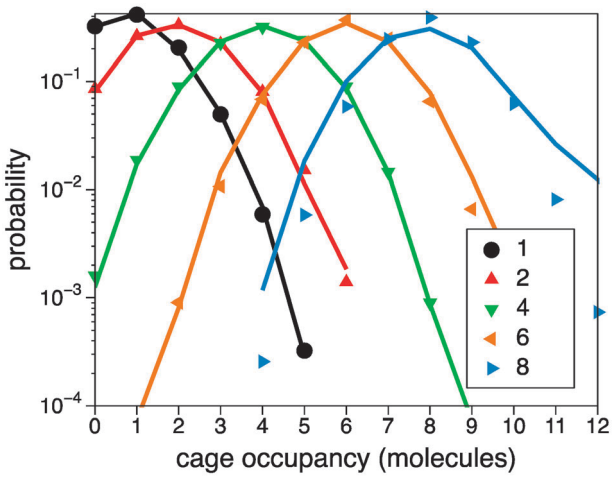

Fig. 5 Cage occupancy probability for different average loadings (molecules per cage, see legend) of methane in LTA at 300 K. Points indicate data from Canonical Monte Carlo simulations, while lines indicate data from simulations of the first kMC model.

loadings, but begin to disagree at an average loading of eight particles per cage.

Fig. 6 compares the self-diffusion coefficients of methane in LTA at 300 K as obtained using MD, the analytical expressions which account for concentration fluctuations implicitly and explicitly (see Section 2.4), and the values obtained by Beerdsen *et al.*[19] using the implicit treatment of concentration fluctuations. Quantitative agreement is observed at most loadings, in particular at loadings below the key concentration of nine molecules per cage.

4.1.4 Kinetic Monte Carlo. The self- and collective-diffusion coefficients of methane in LTA at 300 K were obtained using MD and kMC simulations (Fig. 8). In the first type of kMC simulation, in which a lattice site represents an entire super-cage, no separation is seen between D_S and D_C. This replicates the behavior observed from MD at low loadings. However, at higher loadings, a second type of kMC simulation becomes necessary, since more local maxima are observed in the probability density (Fig. 2). This second kMC model consisted of a $3 \times 3 \times 3$ cube of super-cages, each subdivided into fifteen lattice sites[13] (Fig. 7): one "A" site in the center, eight "B" sites arranged as vertices of a cube around that, and six "C" sites arranges as faces of the cube around those. The central "A" site is connected to the eight adjacent "B" sites, which are each connected to the nearest three "C" sites. Each "C" site is also connected to the nearest "C" site of the adjacent super-cage. Each of these lattice sites can accommodate at most one particle. The hop rates between these sites were defined as

$$K_{\text{hop}} = \begin{cases} 0 & \text{if occupied} \\ K_{\text{TST}} & \text{if unoccupied} \end{cases}$$

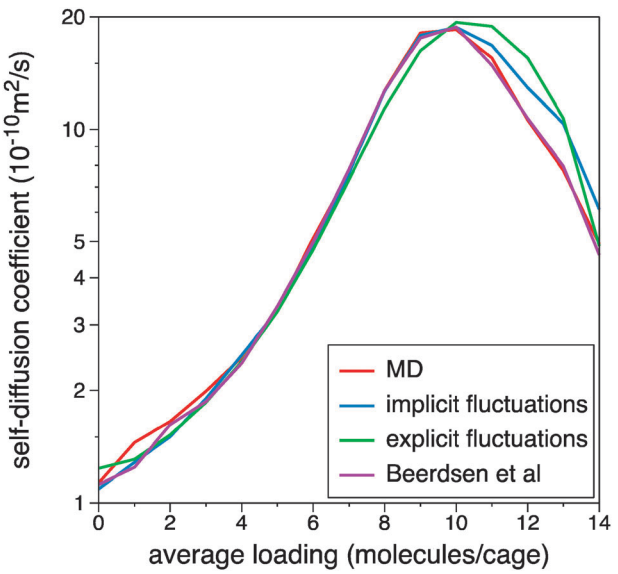

Fig. 6 Self-diffusion coefficient of methane as a function of loading in LTA at 300 K from MD, random walk theory using data from cages with an imposed average loading, random walk theory with explicit concentration fluctuation contributions as presented in this paper, and the values found by Beerdsen *et al.*[19]

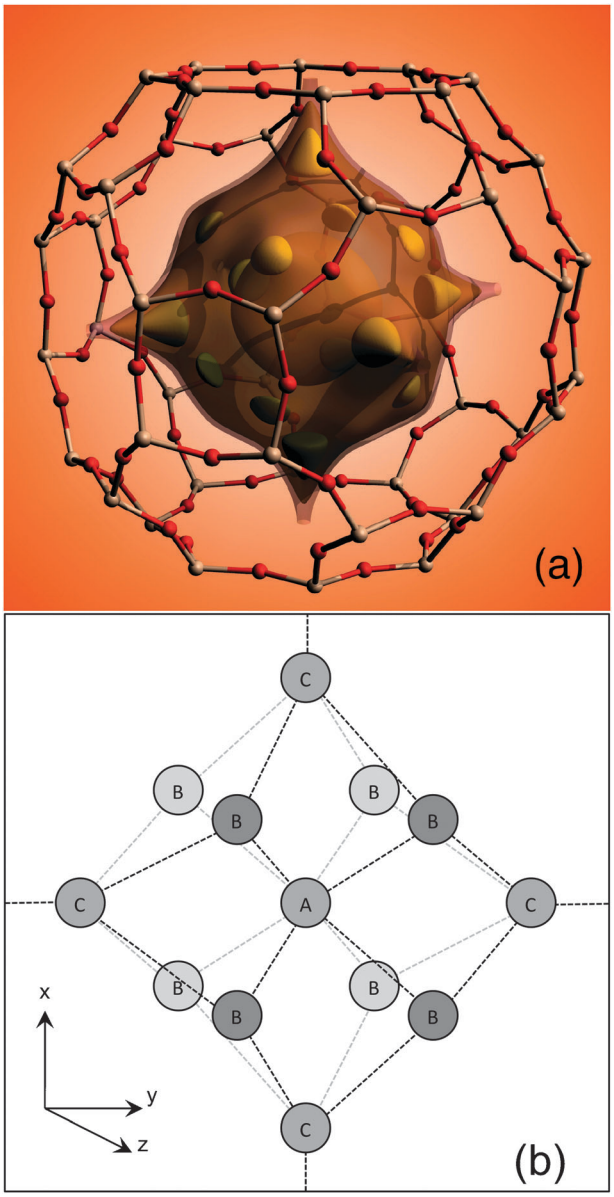

Fig. 7 (a) Free energy surfaces of methane in zeolite LTA at 300 K. Three types of local minima are observed, as described in the text. (b) Schematic of sub-cage adsorption lattice sites comprising one super-cage of LTA. Each "C" site is connected to the nearby "C" sites of a neighboring super-cage (for clarity, the two "C" sub-cage sites in line with the central "A" site along the z-direction are omitted).

where

$$K_{\text{TST}} = \nu_B \times \frac{e^{-\beta F(\text{barrier})}}{\int_{\text{sub-cage}} e^{-\beta F(x)} dx.}$$

The re-crossing coefficient is accounted for in the definition of K_{hop} above, where the particle is effectively barred from entering an occupied site. This second model qualitatively replicates the separation between D_S and D_C observed in the MD simulation, but quantitatively is not in perfect agreement.

4.2 Zeolites SAS and AFI: asymmetrical re-crossing coefficients

In zeolite SAS, the re-crossing coefficient was calculated for methane at 300 K (Fig. 9). Modeling the asymmetrical re-crossing coefficients as the harmonic mean of the two symmetrical re-crossing coefficients gives a correlation coefficient of 0.995.

In zeolite AFI, the re-crossing coefficients of helium at 300 K were computed (Fig. 10). The predicted value from the model (eqn (11)) gives quantitative agreement as long as there are three or fewer particles in each cage.

4.3 Diffusion of isobutane in zeolite MFI

In zeolite MFI, isobutane was analyzed in detail at 600 K. From Canonical MC simulations, the probability density distribution was calculated (Fig. 11) in both the x and y directions at infinite dilution. This information was used to calculate TST hop rates of the molecules between sites. Two different models were considered for this system. In the first model, the molecules were thought to move from intersection to intersection, spending a negligible amount of time between intersection sites. In the second model, two additional sites were considered in each channel, corresponding to the local free energy minima observed there.

Several Bennett–Chandler simulations were executed, constraining the central pseudo-atom of isobutane to the central barrier of either channel type, and allowing the simulation to run until that pseudo-atom reached either adjacent intersection. This characterizes the hop rate between intersection sites. However, for the more finely detailed model, four more Bennett–Chandler simulations were executed, one for each of the barrier types: intersection to x channel site, intersection to y channel site, x channel site to x channel site, and y channel site to y channel site. The re-crossing coefficients for this system were low enough to indicate that the barrier crossings

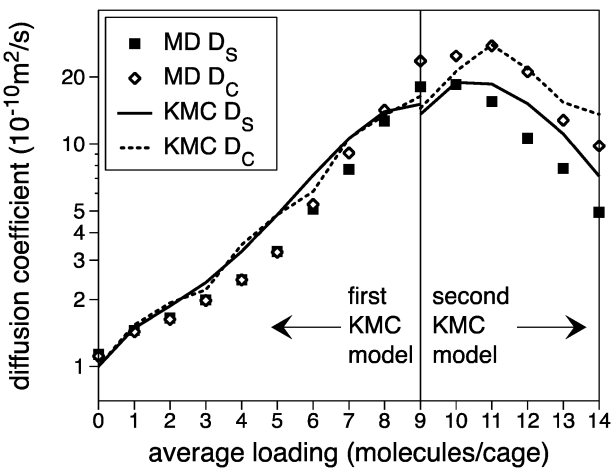

Fig. 8 Self- and collective-diffusion coefficients of methane as a function of loading in LTA at 300 K. Points are from MD simulations, lines are from the kMC models. For loadings up to nine molecules per cage, the results of the first kMC model (large super-cages with perfect mixing) are shown. For loadings at nine and above, results from the second kMC model are shown (fifteen discrete lattice sites within a super-cage, as shown in Fig. 9).

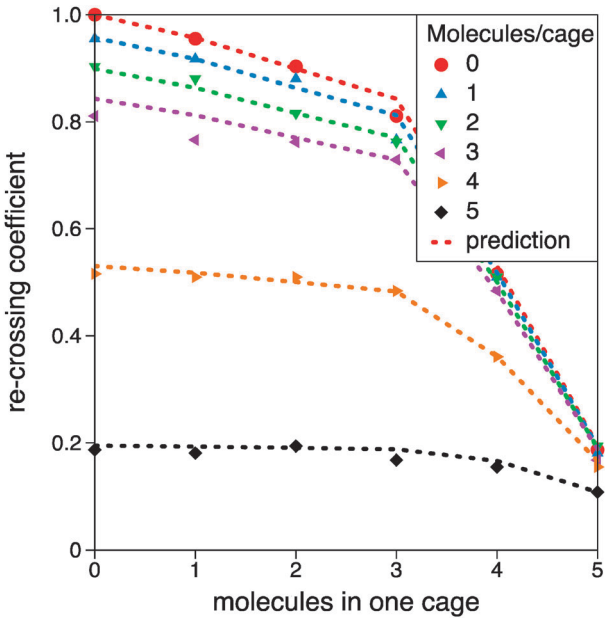

Fig. 9 Re-crossing coefficients of methane in SAS at 300 K for various loadings in each participating cage. The loading of one cage is indicated on the x-axis, and the loading of the other cage is indicated in the legend. Symbols are data from explicit Bennett–Chandler simulations, while lines are the predictions of the model presented in this work.

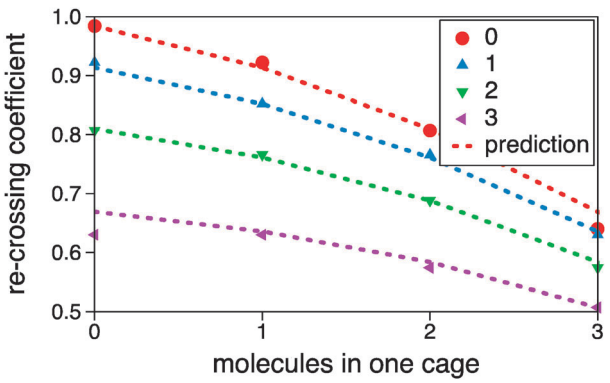

Fig. 10 Re-crossing coefficients of helium in AFI at 300 K for various loadings in each participating cage. The loading of one cage is indicated on the x-axis, and the loading of the other cage is indicated in the legend. Points are data from explicit Bennett–Chandler simulations, while lines are the predictions of the model presented in this work.

may be diffusive, suggesting a possible application of the more-efficient treatment laid out by Frenkel and Smit.[21]

KMC simulations were run for either model type based only on the hop rates obtained from Canonical MC and BC simulations run at infinite dilution. In the more-detailed model, we did not allow both channel-type sites within the same channel to be occupied at the same time, in order to reflect the dynamics of the true system. The resulting self- and collective-diffusion coefficients are shown in Fig. 12, along with results from direct MD simulations. While the central pseudo-atom of the adsorbate was observed to spend only 0.2% of the time in the channels, the associated "passing" behavior is seen to be an important aspect of the overall diffusion activity, as the kMC simulation which disallows it

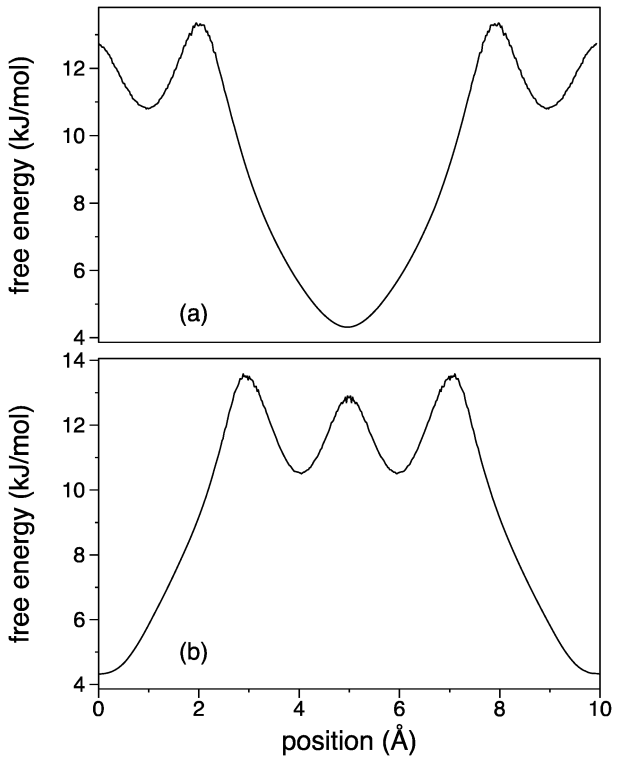

Fig. 11 Free energy profiles of isobutane (central pseudo-atom) in zeolite MFI at 600 K. Fig. 12(a) shows the profile in the *y*-direction, and Fig. 12(b) shows the profile in the *x*-direction.

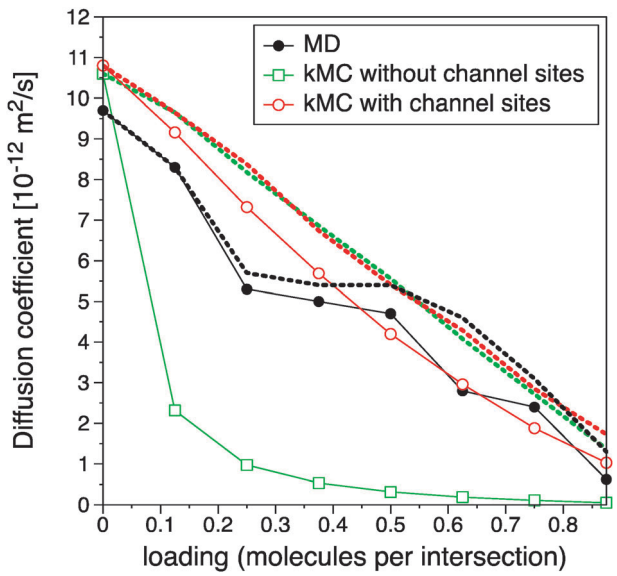

Fig. 12 Self- and collective-diffusion coefficients of isobutane in zeolite MFI at 600 K. Solid lines represent self-diffusion coefficients and dotted lines represent collective-diffusion coefficients.

has an exaggerated D_C/D_S separation compared to MD, but one which accounts for it has a closer D_C/D_S separation, corresponding more closely to the MD simulation. Quantitatively, the kMC with channel sites offers a correlation coefficient of 0.89 to the MD for the self-diffusion coefficient. These diffusion coefficient values are near the reported values for this system,[34–36] although the system is known to be sensitive to force-field parameters[37] and the rigidity of the framework.[38]

5. Conclusions

The mixing rule for asymmetric re-crossing coefficients is seen to be quantitatively accurate in systems where the assumptions of that model are upheld. Some systematic deviations between the observed results and the model's predictions occurred in each system at a high enough adsorbate density to nullify the model's assumptions.

The D_S results from the analytical expression that explicitly accounts for fluctuations in cage loading agree in the LTA system quantitatively with the results of MD, and with the results of the analytical expression that implicitly accounts for such fluctuations. The hop rates obtained with this method are necessary to run a kMC simulation that includes particle interactions, so that the microscopic fluctuations are properly accounted for.

In the LTA system, the separation between D_S and D_C at higher loadings was shown to be a result of a change in adsorbate packing behavior, demonstrated by the local minima that developed in the free energy at those loadings. Until then the particles in a super-cage were reasonably well mixed, with no correlation between a particle's previous cage and next cage. But at higher loadings, a particle is detained at various distinct adsorption sites within a cage, leading to these correlations and thus the separation between the self- and collective-diffusion behaviors. This change in behaviors was demonstrated in the two kMC simulations, one which assumes each cage is well-mixed, finding that $D_C = D_S$, and the other which subdivides the cage into smaller sites to allow a stronger interaction between particles, finding that that $D_C > D_S$. This phenomenon is further demonstrated with isobutane in MFI, where the kMC simulations replicate the D_C/D_S separation observed with MD. Even more encouraging is the fact that, for isobutane in MFI, quantitatively close predictions of both the self- and collective-diffusion properties at high loadings are obtained from kMC simulations that use only the hop rates calculated at infinite dilution.

Acknowledgements

The authors would like to thank Dr Richard Luis Martin for allowing us to use his image (Fig. 7a). MKFA was supported by the Advanced Research Projects Agency–Energy (ARPA-E), U.S. Department of Energy. BS was supported as part of the Center for Gas Separations Relevant to Clean Energy Technologies, and Energy Frontier Research Center funded by the U.S. Department of Energy, Office of Science, Office of Basic Energy Sciences under Award Number DE-SC0001015.

Notes and references

1 S. Auerbach, K. Carrado and P. Dutta, *Handbook of Zeolite Science and Technology*, Marcel Dekker, New York, 2004.
2 D. M. D'Alessandro, B. Smit and J. R. Long, *Angew. Chem., Int. Ed.*, 2010, **49**, 6058–6082.
3 K. Sumida, D. L. Rogow, J. A. Mason, T. M. McDonald, E. D. Bloch, Z. R. Herm, T.-H. Bae and J. R. Long, *Chem. Rev.*, 2012, **112**, 724–781.

4 J.-R. Li, J. Sculley and H.-C. Zhou, *Chem. Rev.*, 2012, **112**, 869–932.
5 B. Smit and T. L. M. Maesen, *Chem. Rev.*, 2008, **108**, 4125–4184.
6 M. W. Deem, R. Pophale, P. A. Cheeseman and D. J. Earl, *J. Phys. Chem. C*, 2009, **113**, 21353–21360.
7 E. Haldoupis, S. Nair and D. S. Sholl, *Phys. Chem. Chem. Phys.*, 2011, **13**, 5053–5060.
8 B. Smit and R. Krishna, *Chem. Eng. Sci.*, 2003, **58**, 557–568.
9 R. L. June, A. T. Bell and D. N. Theodorou, *J. Phys. Chem.*, 1991, **95**, 8866–8878.
10 H. Eyring, *J. Chem. Phys.*, 1935, **3**, 107–115.
11 C. Bennett, *Diffusion in Solids: Recent Developments*, Academic Press, New York, 1975, pp. 73–113.
12 D. Chandler, *J. Chem. Phys.*, 1978, **68**, 2959–2970.
13 E. Beerdsen, B. Smit and D. Dubbeldam, *Phys. Rev. Lett.*, 2004, **93**.
14 R. Krishna, D. Paschek and R. Baur, *Microporous Mesoporous Mater.*, 2004, **76**, 233–246.
15 D. A. Reed and G. Ehrlich, *Surf. Sci.*, 1981, **105**, 603–628.
16 K. A. Fichthorn and W. H. Weinberg, *J. Chem. Phys.*, 1991, **95**, 1090–1096.
17 S. E. Jee and D. S. Sholl, *J. Am. Chem. Soc.*, 2009, **131**, 7896–7904.
18 D. Dubbeldam, E. Beerdsen, T. J. H. Vlugt and B. Smit, *J. Chem. Phys.*, 2005, **122**, 224712.
19 E. Beerdsen, D. Dubbeldam and B. Smit, *J. Phys. Chem. B*, 2006, **110**, 22754–22772.
20 D. Dubbeldam, E. Beerdsen, S. Calero and B. Smit, *J. Phys. Chem. B*, 2006, **110**, 3164–3172.
21 D. Frenkel and B. Smit, *Understanding Molecular Simulation*, Academic Press, San Diego, CA, 2 edn, 2002, vol. 1.
22 J. Karger and D. Ruthven, *Diffusion in Zeolites and Other Microporous Solids*, John Wiley and Sons, Inc., USA, 1992, pp. 23–25.
23 D. Dubbeldam, S. Calero, T. J. H. Vlugt, R. Krishna, T. L. M. Maesen, E. Beerdsen and B. Smit, *Phys. Rev. Lett.*, 2004, **93**.
24 D. Dubbeldam, S. Calero, T. J. H. Vlugt, R. Krishna, T. L. M. Maesen and B. Smit, *J. Phys. Chem. B*, 2004, **108**, 12301–12313.
25 O. Talu and A. L. Myers, *AIChE J.*, 2001, **47**, 1160–1168.
26 H. Vankoningsveld, H. Vanbekkum and J. C. Jansen, *Acta Crystallogr., Sect. B: Struct. Sci.*, 1987, **43**, 127–132.
27 S. P. Bates, W. J. M. vanWell, R. A. vanSanten and B. Smit, *J. Am. Chem. Soc.*, 1996, **118**, 6753–6759.
28 N. E. R. Zimmermann, S. Jakobtorweihen, E. Beerdsen, B. Smit and F. J. Keil, *J. Phys. Chem. C*, 2007, **111**, 17370–17381.
29 S. Nose, *J. Chem. Phys.*, 1984, **81**, 511–519.
30 W. G. Hoover, *Phys. Rev. A: At., Mol., Opt. Phys.*, 1985, **31**, 1695–1697.
31 L. Verlet, *Phys. Rev.*, 1967, **159**, 98–&.
32 N. Metropolis, A. W. Rosenbluth, M. N. Rosenbluth, A. H. Teller and E. Teller, *J. Chem. Phys.*, 1953, **21**, 1087–1092.
33 D. T. Gillespie, *J. Phys. Chem.*, 1977, **81**, 2340–2361.
34 R. Krishna and R. Baur, *Sep. Purif. Technol.*, 2003, **33**, 213–254.
35 C. Chmelik, L. Heinke, J. Kaerger, W. Schmidt, D. B. Shah, J. M. van Baten and R. Krishna, *Chem. Phys. Lett.*, 2008, **459**, 141–145.
36 B. Millot, A. Methivier, H. Jobic, H. Moueddeb and M. Bee, *J. Phys. Chem. B*, 1999, **103**, 1096–1101.
37 T. J. H. Vlugt, C. Dellago and B. Smit, *J. Chem. Phys.*, 2000, **113**, 8791–8799.
38 A. Bouyermaouen and A. Bellemans, *J. Chem. Phys.*, 1998, **108**, 2170–2172.